

A Study of the Dynamics of Soil Erosion Using Rusle2 Modelling and Geospatial Tool in Edda-Afikpo Mesas, South Eastern Nigeria



Joseph I. Amah*, Okechukwu P. Aghamelu, Olufemi V. Omonona, Ikechukwu M. Onwe

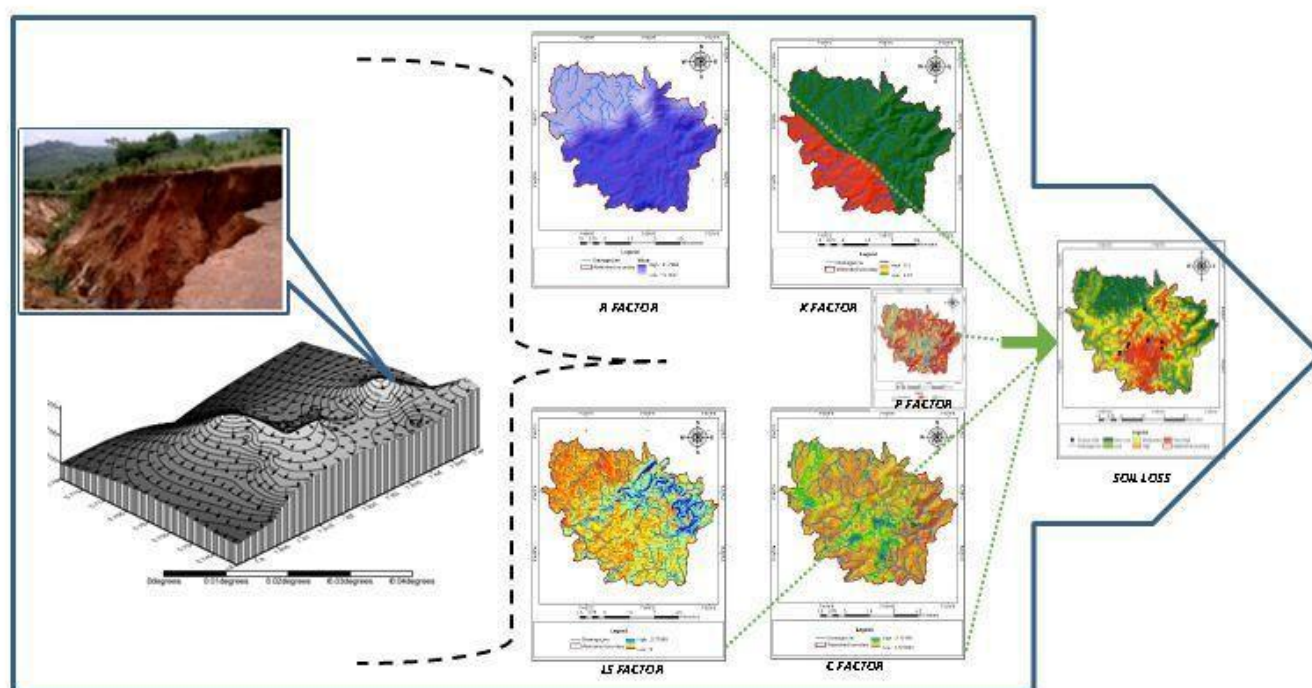
Department of Physics, Geology and Geophysics, Alex Ekwueme Federal University, Ndufu-Alike, PMB 1010, Abakaliki, Nigeria.

*Corresponding Author Email: amahdejoe@yahoo.com

DOI: 10.2478/pjg-2020-0007

Abstract:

The Revised Universal Soil Loss Equation (RUSLE) was used to study the soil erosion processes in Edda-Afikpo mesas, Lower Cross River watersheds, Nigeria. The mesas occupy an area estimated at 60km² on a surface relief of about 284m. DEM data, satellite images and basemap of the area were used. Remotely sensed data were ground-truthed through extensive field works. The results show that the process is facilitated by the Trifecta of hill slope hydrology, geology and land use practices. Steep hill Slope of values 78 % at the major hot spots, very fragile, dry and non-plastic sandy soils all aid sediment detachment. Analysis of the index properties which include Liquid Limit(LL) of 25-30, moisture content(w%) of 5.9-7.4, permeability of $1.541 \times 10^{-3} - 1.636 \times 10^{-3}$ cm/s and shear strength of 36-42 KN/m² predispose the sediments to detachment and erosion. Based on the analysis, the amount of soil loss in the project area is about 1373.79 ton per year. Soil erosivity factor is high at the mesas ($5023.83 \text{ MJ mm ha}^{-1} \text{ h}^{-1} \text{ yr}^{-1}$ - $5069.51 \text{ MJ mm ha}^{-1} \text{ h}^{-1} \text{ yr}^{-1}$) The sandy layer attain thickness of 50m-60m in places and with high pore pressure development, slope failure are triggered during intense storm events. In terms of vulnerability level in erosion risk, high to very high constitute 4.1% of the watershed which translate to 5.05km² of the 59km². The various processes occur simultaneously and are exacerbated by human factors through seasonal bush burning and development along drainage lines. The study reveals that 18.8% of the available land for development is at high to very high risk of erosion. The soil loss model has been validated and the hotspots from the map coincide with the gully sites. The results of this research can therefore be used for conservation and adaptation purposes.



Keywords: Land use, GIS, landscape, Hydrology, soil erosion, model.

1.0. Introduction

The southeastern part of Nigeria has a history of environmental problems that has been in the public domain in recent times. Most parts of this area, according to Ofomata, are underlain by geological formations that are prone to soil erosion [1]. A typical example of one of those areas of southeastern Nigeria is Edda-Afikpo. The mass wasting processes in this locality manifest in the form of landslides and slumping most often triggered by rainfall and storm events on the weak exposed soil. The spatial extent and severity, however, remains to be sufficiently documented. Among factors that were identified to contribute to physical degradation of an area are topography, geology and climate, pattern of precipitation, and land use practices. The degradation of the area which comprises Nguzu and Ekoli settlements and their environs, all in Afikpo South of Ebonyi State, Nigeria, has elicited national attention.

The Revised Universal Soil Loss Equation by Renard et al was used in this study to quantify the volume of soil loss in the watershed [2]. Assessment of soil loss in large areas are often difficult due to its isolated and heterogeneous nature. As a result, traditional methods of mapping soil erosion are very challenging. Some group researchers indicate that integrating soil erosion model and geographic information system (GIS) techniques makes soil erosion estimation spatially feasible, cost-effective and accurate [3-5]. So submits that integrating RUSLE2 with GIS could be used to develop a spatial decision support system to estimate soil loss under different conservation practices and used to implement conservation planning in a watershed [6]. The role of land use cover or vegetation cover especially of a woody type with strong root and large root systems in slope stability have been documented by various researchers [7-9].

The objectives of the study are: (i) to develop a proactive measure to mitigate the gully and soil loss processes by identifying hotspots and predisposing factors, instead of the hitherto reactive option adopted by government authorities and the stakeholders. (ii) identify the roles played by the various factors in the mass wasting processes. (iii) Bring into focus how human activities contribute to the disasters and make a case for attitudinal change; and (iv) Suggest

workable adaptive or mitigation measures that could be enforced by planning and conservation authorities from the identified causal factors. This study aims to solve the erosion problems through providing answers to the following questions: (i) can a model be developed to examine the degradation of Edda on a spatial scale in view of the ineffectual remediation in place? (ii) what research efforts can best guide the conservation authorities to adopt quantitative and qualitative measures to save Edda from further degradation?

1.1. The Study area.

The study was conducted in Afikpo South Local government of Ebonyi State, Southeastern Nigeria.

1.2. Location and accessibility

Geographically, the Edda area, which serves as the study area, is located in southeastern Nigeria. It is bounded by latitudes $5^{\circ} 45' N$ and $5^{\circ} 49' N$ and longitudes $7^{\circ} 49' E$ and $7^{\circ} 53' E$. It is located at the southern boundary of the Afikpo Syncline and forms part of the Lower Cross River watershed (Figure 1). It is a mesa at the top of which the Nguzu-Edda and other settlements lie. The area is accessed through the Afikpo - Okigwe, Amasiri - Owutu-Edda - Nguzu-Edda, Nguzu-Edda - Ohafia, and Nkporo - Okigwe Roads.

1.3. Climate and rain fall pattern

Two main seasons characterize the climate, the dry season which lasts from November to March and the rainy season which begins in April and ends in October with a short period of reduced rains in August commonly referred to as "August break". Temperature in the dry season ranges from 22 to $36^{\circ}C$, and results in high evapo-transpiration, while during the rainy season temperature ranges from 16 to $28^{\circ}C$, with generally lower evapo-transpiration. The average monthly rainfall ranges from 31 mm in January to 270 mm in July, with the dry season experiencing much reduced volume of rainfall unlike the rainy season, which has high volume of rainfall. Average annual rainfall is estimated at 2022 mm (Figure 2).

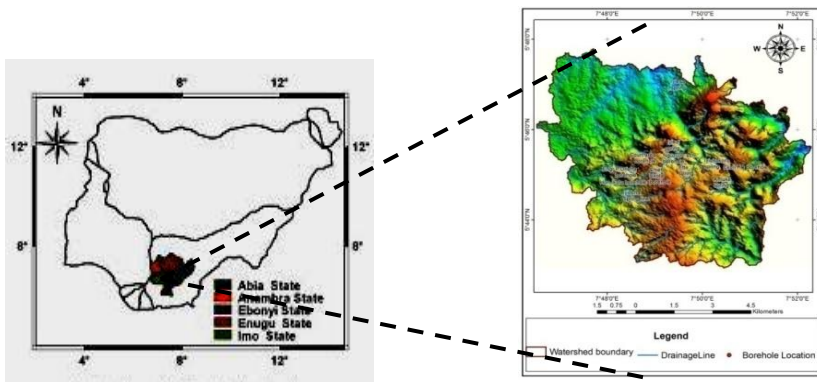


Figure 1: Study area - Lower Cross River Watershed, Nigeria.

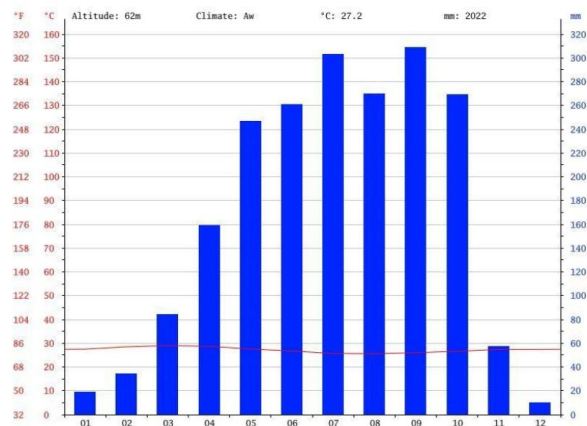


Figure 2: Temperature and rainfall pattern in Edda area.



Figure 3: Gully erosion sites at Nguzu (near Local Government Secretariat)

2.0. Physiographic Setting

The topographic elevations of the area peak at 282m and decrease to a minimum of 90m at the adjoining lowlands (see Figure 4). This plateau surface is actively undergoing rapid modifications by erosion on all sides resulting in deep incised gullies. Springs issue out from the highlands at about 165-125m and drain down the low areas, further cutting into the landscape and draining into the Afikpo synclinorium with elevation minima as low as 30m. Climatic and physiographic characteristics affect the pattern of disposal of stream flow which transports the sediments.

The numerous streams radiate away from a central region indicating the controlling influence of a central highland such as an eroding pluton surrounded by sedimentary rocks. The drainage pattern of the individual tributaries follows dendritic patterns underscoring the flat-lying sedimentary rocks which is homogeneous and uninterrupted by fractures. First and second order streams dominate the watershed. First to third order streams are generally found in the upper reaches of a watershed. The drainage is controlled by the relief and geology. The valleys host perennial streams giving rise to wetlands with heavy sediment loads and few ephemeral streams with dry channels. These wetlands are thickly wooded while the slopes and uplands are sparsely vegetated. The two main Campano-Maastrichtian formations found in the area are the Nkporo and Owutu Sandstone (a lateral equivalent of highly friable and deeply unconsolidated Ajali Sandstone).

The Nkporo Shale was deposited during the Campano-Maastrichtian period, which began with a short marine transgression followed by regression. The formation consists mainly of dark-gray shales with occasional thin beds of sandy shale and sandstone, resting unconformably on the Albian-Santonian sediments of Abakaliki Fold Belt. The Owutu Sandstone was a product of marine regression during the Maastrichtian. The formation consists of sandstones, shales and sandy shales. The sandstones components are fine to medium grained and yellow to white in color.

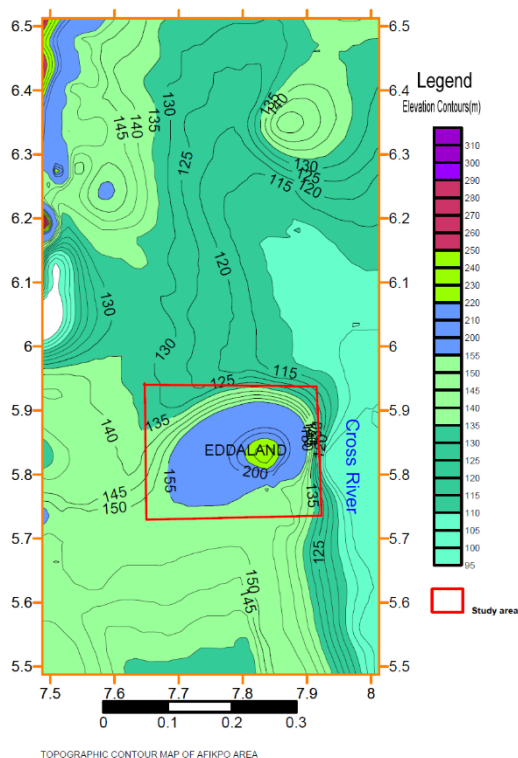


Figure 4: Topographic map of the study area

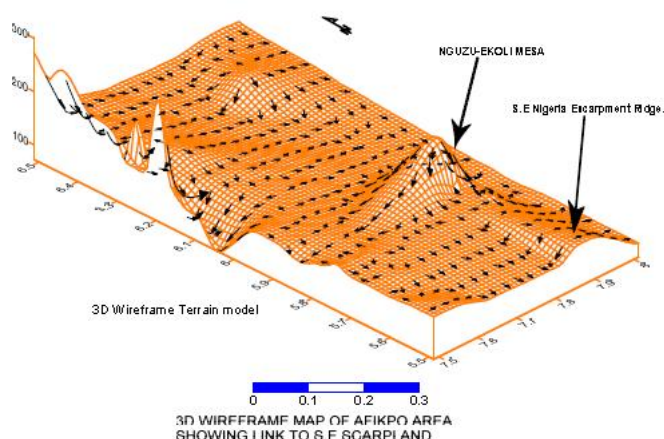


Figure 5: Terrain model of the study area showing the mesas.

3.0. Materials and methods

3.1. Data Inventory

The study involved field work for ground-truthing of satellite images and digital elevation model (DEM) data. The geologic hardware used included a global positioning system (GPS) device model GARMIN VENTURE HC etrex with inbuilt compass and route tracking capability, geologic hammer, hand auger, sampling containers, Topographic base map of Afikpo South. Table 1 summarizes the spatial and temporal data used: (1) Soil data (2) SRTM 30m Digital Elevation Model (3) Landsat data (4) Rainfall/precipitation data (5) Conservation practices data (6) State, county, watershed and sub watershed boundary data (7) Feature location data with GPS readings. SRTM 30m DEM of the study area was downloaded and was in datum WGS84 on the 20th June 2017 [10]. The data was projected to the UTM coordinate system and clipped to the extent of the project area. It provided the elevation data needed to generate the terrain parameters needed for ArcGIS models for L and S factors (slope length and slope steepness) required for Revised Universal Soil Loss Equation (RUSLE2). For the purpose of sub-setting of the study area, an existing shape file of the study area for 2017 was obtained from the Office of the Surveyor General of the Federation. Its co-ordinate system was checked, and it conformed to Universal Transverse Mercator (UTM) Zone 32N, WGS 1984. Table 1 is an inventory of the data used for the study.

Table 1: Data, description and sources

| S/N | TYPE | FORMAT | SCALE/ RESOLUTION | DATE/SOURCE |
|-----|-------------------------------|----------|-------------------|--------------|
| 1 | Soil map | Analogue | 1:250,000 | [2] |
| 2 | Landsat Sat. Imagery | Digital | 30m | 2017/ Glovis |
| 3 | SRTM Elevation data | Digital | 30m | USGS |
| 4 | Isoerodent data | Digital | | [11] |
| 5 | Topographic basemap of Afikpo | Analogue | 1:250,000 | (GSN,1983) |

3.2. Field Work and Data Acquisition.

The stream locations, gully sites were recorded with GPS in an xyz format. Soil samples were collected at the gully sites with a 4-inch hand-auger, at depths between 1 and 1.5 m. The GPS elevation data were compared with contour values on the base map and certified. Tables 1 and 2 show the data sources and field data acquired for the study while Table 3 is a summary of computed parameters for the study. The soil samples were carefully collected and sent for laboratory tests. Sampling and testing of the soil samples followed British standard specifications. The tests included grain size distribution, Atterberg limits, natural moisture contents and specific gravity and shear strength.

Table 2: Description of landmarks and sampling points

| Feature | Longitude(E) | Latitude(N) | Elevation(m) | Remark/data |
|--|---------------|---------------|--------------|-------------------------------|
| IkOta's residence Nguzu | 7.8135 | 5.7488 | 169 | Landmark/borehole data |
| Kingsley Ezeudu residence | 7.8128 | 5.7472 | 176 | Borehole data |
| Former Afikpo South Council Headquarters | 7.8255 | 5.7511 | 213 | Landmark/soil sampling |
| Double Corner gully site | 7.8241 | 5.769 | 130 | Landmark/soil sampling |
| Iyiesa stream | 7.8223 | 5.7802 | 69 | Landmark/spring line |
| Iyiocha downstream | 7.7963 | 5.7443 | 109 | Landmark/spring line |
| Iyiocha upstream | 7.8045 | 5.7399 | 120 | Landmark/spring line |
| IgboroAmojigully site | 7.8077 | 5.7418 | 159 | Landmark/soil sampling |
| Igboro AMORJI peak | 7.8125 | 5.7475 | 172 | Landmark |
| Iyiokpa spring | 7.8152 | 5.7562 | 168 | Landmark/spring line |
| Iyintoala stream | 7.8112 | 5.7513 | 145 | Landmark/spring line |
| Court area borehole | 7.8175 | 5.7587 | 188 | Landmark/borehole data |
| Chief Ukota borehole | 7.8137 | 5.7525 | 181 | Landmark/borehole data |
| Engr P.Orioha borehole | 7.8103 | 5.7479 | 158 | Landmark/borehole data |
| Honourable Ikota borehole | 7.8138 | 5.7487 | 172 | Landmark/borehole data |

| | | | | |
|-------------------------------|--------|--------|-----|------------------------|
| Nguzu Primary School borehole | 7.8185 | 5.7536 | 190 | Landmark/borehole data |
| Afikpo South Local Government | 7.8258 | 5.7512 | 203 | Landmark |
| Ekoli development centre | 7.8372 | 5.7464 | 191 | Landmark |
| Nguzu-Ohafia road gully site | 7.8347 | 5.746 | 179 | Soil sampling |
| Alioma road gully site | 7.8353 | 5.75 | 180 | Soil sampling |
| Iyiezi spring | 7.8263 | 5.7578 | 125 | Landmark/spring line |
| Ette spring | 7.825 | 5.7545 | 152 | Landmark/spring line |
| Amuke spring | 7.8363 | 5.7449 | 167 | Landmark/spring line |
| Iyiokokoro spring | 7.8336 | 5.7512 | 152 | Landmark/spring line |
| Ekoli HC borehole | 7.8399 | 5.7512 | 206 | Landmark/spring line |

Table 3: Summary of Computed Parameters used for the study based on published authorities.

| S/ N | Parameters | Definition | Unit | References |
|---------|--|--|-----------------|------------|
| 1. | Area(m) | Geographic area of watershed | km ² | |
| 2. | Basin Relief(Rb) | $R = H-h$, where H is the maximum elevation and h is the minimum elevation within the basin | M | [12] |
| 3 | Basin Slope(Sb) | $Sb = \left(\frac{M \times N}{A} \right) \times 100$ where M is the total length of the contours within the watershed in meters, N the contour interval in meters and A is the basin area in m ² | % | |
| 4 | Stream Length(Lu) | Length of the major stream | Km | [13] |
| 5 | Stream Order(Nu) | Hierachical ordering | Km | [13] |
| 6 | Basin length(Lb) | Maximum length of basin measured parallel to the main drainage line | Km | |
| 7 | Hydraulic head(H) | Elevation of datum(m)-waterlevel(m) | M | |
| 8 | Slope length(L) | The ratio of soil loss from the field slope length to that from 72.6ft length under identical conditions | Unitless | [2] |
| 9 | Slope steepness(S) | Ratio of soil loss from the field slope gradient to that from a 9% slope under identical conditions | | [9] |
| 10 | Computed Spatial average soil Loss (A) | $A = R \times K \times L \times S \times C \times P$ Where, the variables are as defined in RUSLE2. | Ton/ha/yr | [14] |

3.3. Data processing and software used for the study.

The set of software used in data processing and analysis is listed below. This set of software has the capabilities to do the following: linear enhancement, land-use classification, watershed processing, statistical analysis and terrain modelling.

i. Erdas Imagine software: it was used for image enhancement, Landsat processing and NDVI analysis of the project area.

ii. Global mapper 16.1: it was used for clipping and data conversion from one format to another

iii. ArcGIS 10.3: it was used for data integration.

The software is packaged with a powerful collection of spatial analytical extensions that was also used for mapping and geospatial analysis. This software was used for RUSLE integration, Data visualisation, layout design, contour generation, hydro analysis and terrain analysis. A geo-database was set up in arc catalog with the above feature classes. This was deployed to ArcMap with the STRM 30M DEM of the area used as basemap. The model runs were done stepwise from terrain preprocessing to hydro network generation. A digitized basemap of the area was used to ground truth the DEM and the shape of the study area clipped to the DEM. The results are shown in Figs 9-14 and Tables 5-10. v. Surfer 10.3. This software was used to model the terrain and topography of the study area for visual purposes. The data for this came from the digital elevation model dataset and complimented with data acquired from the field exercise.

3.4. Terrain models

The elevation data extracted from the DEM was used to prepare a work sheet and grid in surfer 10.3. The topographic contour map and 3D terrain models were made from this. The maps are intended to enhance spatial understanding of the study area and highlight specific features in the area (Figs 4 and 5).

3.5. Soil Loss assessment with RUSCLE2

The RUSLE2 model was used in a GIS platform in this study [2]. The RUSLE2 is an improvement of earlier version and was designed to compute the mean annual soil loss for ground slopes where flow convergence/divergence is minimal as can be obtained in agricultural lands. The RUSLE is expressed by an equation,

$$A = [R] * [K] * [LS] * [C] * [P], \quad (1)$$

where, A = soil loss ($t\ ha^{-1}\ yr^{-1}$), R = rainfall erosivity factor ($MJ\ mm\ ha^{-1}\ h^{-1},\ yr^{-1}$), K = soil erodibility factor ($t\ h\ MJ^{-1}\ mm^{-1}$), LS = slope-length and slope steepness factor (dimensionless), C = land management factor (dimensionless), and P = conservation practice factor (dimensionless).

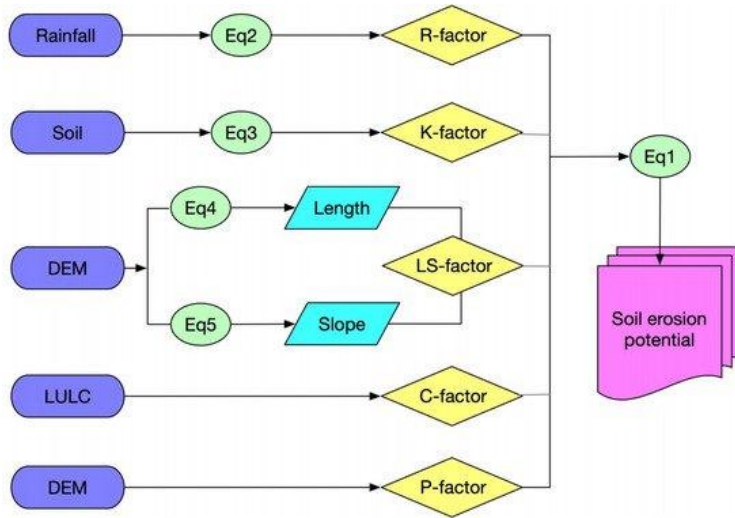


Figure 6: The methodological framework of implementing the RUSLE model for soil erosion estimation [15].

3.5.1. RUSLE Parameters Computation

Rainfall-Runoff Erosivity Factor (R).

The rainfall – runoff erosivity factor is defined as the mean annual sum of individual storm erosion index values, EI_{30} , where E is the total storm kinetic energy and I_{30} is the maximum rainfall intensity in 30 minutes. To compute storm EI_{30} , continuous rainfall intensity data are needed. Wischmeier and Smith found that the best predictor of rainfall erosivity factor (R) was:

$$R = \frac{1}{n} \sum_{j=1}^n \left[\sum_{k=1}^m (E)(I_{30})_k \right] \quad (2)$$

Where: R = rainfall-runoff erosivity factor. E = the total storm kinetic energy in hundreds of ft-tons per acre; I_{30} = the maximum 30-minute rainfall intensity; j = the counter for each year used to produce the average; k = the counter for the number of storms in a year; m = the number of storms n each year; n = the number of years used to obtain the average R. The calculated erosion potential for an individual storm is usually designated EI. The total annual R is therefore the sum of the individual EI values for each rainfall storm event. The energy of a rainfall storm is a function of the amount of rain and of all the storm's intensity components. Wischmeier also found that the rain kinetic energy (E) relationship, based on the data expressed by the equation;

$$E = 916 (331) \log_{10} (I), I \leq 3.0 \text{ in/hr}$$

$$E = 1074, I \leq 3.0 \text{ in/hr} \quad (3)$$

Where: I = the average rain intensity; E = the kinetic energy in ft-tons per acre inch of rain

In a prior project implementation, values of rainfall erosivity factor, R, was translated to isoerodent map of Nigeria showing both monthly and annual EI_{30} index according to a study [16]. This facilitated the determination of the required rainfall-runoff erosivity value for the required area. The rainfall erosivity value for the area was then extracted using the isoerodent data which reflects the potential ability of raindrops to cause erosion, the value was divided by 12 (number of months in a year) to arrive at the average annual R factor value and R value map was generated using the triangulation method of interpolation based on kriging technique using ArcGIS 10.3 and converted into a 30m grid to derive the R factor map. This was then clipped into the project area boundary. The rainfall map represents mean annual precipitation over the country, produced from the ground meteorological stations. The equation integrated to generate the R-factor is given.

$$R = 38.5 + 0.35P, \quad (3)$$

where, R = Rainfall Erosivity Factor, P = Mean Annual Rainfall in mm

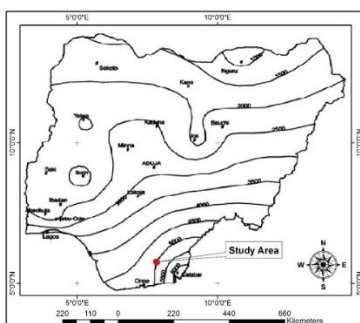


Figure 7: Isoerodent map of Nigeria [16].

3.5.2. Soil Erodibility Factor (K)

Soil erodibility (K) represents the susceptibility of soil or surface material to erosion, transportability of the sediment, and the amount and rate of runoff given a particular rainfall input, as measured under a standard condition. Erodibility varies with soil texture, aggregate stability, infiltration capacity and organic and chemical content. The erodibility textural/parent material parameter is based on a combination of the dominant soil surface texture and the type of parent material. A polygon vector file of the soil map was digitized. This was then rasterised and converted into a K value map by reclassing each soil polygon into its corresponding K value.

Table 4: The K factor value [17].

| Soil Type | K Value |
|---------------------|---------|
| sandy loam surfaces | 0.27 |
| clay surfaces | 0.30 |

3.5.3. Slope Length and Steepness Factor (LS)

The effect of topography on soil erosion is accounted for by the LS factor in RUSLE, which combines the effects of a slope length factor L, and a slope steepness factor S. In general, as slope length (L) increases, total soil erosion and soil erosion per unit area also increase due to the progressive accumulation of runoff in the downslope direction. As the slope steepness (S) increases, the velocity and erosivity of runoff increase. Slope length (L) is defined as the ratio of soil loss from the field slope length to that from a 72.6 ft length under otherwise identical conditions. Figure 8 presents the profile of slope length. For cropping land, L is evaluated by the equations used in RUSLE [18,2] with

$$L = (X_h / 72.6)^m \quad (4)$$

Where: X_h = the horizontal slope length in ft; m = a variable slope length exponent. m is related to the ratio ϵ of rill erosion to inter-rill erosion by the following equation:

$$m = \epsilon / (1 + \epsilon) \quad (5)$$

ϵ is calculated for conditions when the soil is moderately susceptible to both rill and inter-rill erosion using the following equation:

$$\epsilon = \frac{\sin \theta}{0.0896 \times [3.0 \times (\sin \theta)^{0.8} + 0.56]} \quad (6)$$

Where: θ = the slope angle.

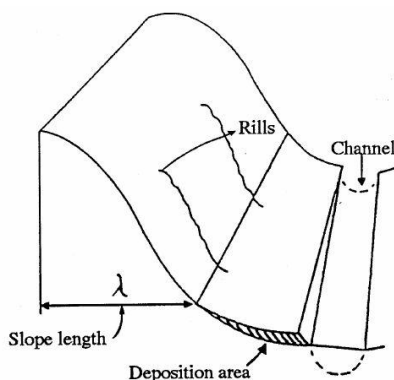


Figure 8: Schematic slope profiles of RUSLE applications [2]

The slope steepness (S) is defined as the ratio of soil loss from the field slope gradient to that from a 9% slope under identical conditions. The RUSLE slope steepness equation is the following [2,18] =

$$10.8 \times \sin \theta + 0.03 \leq 9\%; S = 16.8 \times \sin \theta - 0.50 \geq 9\% \quad (7)$$

Where: θ = the slope angle; σ = the slope gradient in percentage.

The slope length and slope steepness (S) can be defined from the Digital Elevation Model (DEM) [19]. DEM is currently available in 30 meter resolution for

the project area. The LS factor layer is calculated using an Arcinfo AML using the method of [17].

3.5.4. The Cover Factor (C)

The C factor reflects the effects of cropping and management practices on soil erosion rates in agricultural lands and the effects of vegetation canopy and ground covers on reducing the soil erosion in forested regions [2]. To fulfil the task, the excellent and widely used method for crop growth and condition assessment is through the process of NDVI calculation. For this study area NDVI calculation was performed to produce NDVI images for the time period. In addition, the use of spectra vegetation index, namely the Normalized Difference Vegetation Index (NDVI) was also applied to detect areas of vegetation cover. This method has proved reliable in monitoring vegetation change.

Table 5: NDVI Values

| Satellite Imagery | Minimum | Maximum |
|-------------------------|---------|---------|
| Land Sat 8, 2017 | -0.252 | 0.217 |

In order to calculate NDVI, the digital number (DN) in Landsat imagery was converted to spectral radiance and then reflectance for the Near infrared (NIR) band and the Red visible band (RED). The spectral radiance (L) was computed for NIR and RED based on the digital number of each individual pixel. Spectral radiance is the outgoing radiation energy of the band as observed at the top of the atmosphere by the satellite.

The three steps in order to calculate NDVI for Landsat imagery is detailed below:

(i) Conversion from Digital Number to Spectral Radiance

$$L = \frac{(L_{\max} - L_{\min}) * (Q_{cal} - Q_{cal \min})}{(Q_{cal \max} - Q_{cal \min})} + L_{\min} \quad (8)$$

Where : L = Spectral radiance at the sensor aperture (watt m⁻² ster⁻¹ μm⁻¹); L_{max} = Spectral radiance scaled to Q_{calmax} (watt m⁻² ster⁻¹ μm⁻¹); L_{min} = Spectral radiance scaled to Q_{calmin} (watt m⁻² ster⁻¹ μm⁻¹) Q_{cal} = Quantized calibrated pixel value = DN; Q_{calmin} = Minimum quantized calibrated pixel value corresponding to L_{min}; Q_{calmax} = Maximum quantized calibrated pixel value corresponding to L_{max}. L_{max} and L_{min} value was acquired from Landsat post calibration dynamic range table

(ii) Conversion from radiance to reflectance (at-satellite reflectance)

$$r = \frac{\pi * L * d^2}{E_{sun} * \cos \theta * dr} \quad (9)$$

Where: r = Planetary reflectance (unitless); L = Spectral radiance at the sensor aperture (watt m⁻² ster⁻¹ μm⁻¹) dr = Inverse square of earth-sun distance (astronomical unit). E_{sun} = Mean solar exoatmospheric irradiances (watt m⁻² μm⁻¹, Table 2) .θ = Solar zenith angle (degree).

(iii) Computing NDVI using Landsat bands in reflectance NDVI is computed using below formula:

$$NDVI = \frac{rNIR - rRed}{rNIR + rRed} \quad (10)$$

where rNIR is the reflectance value in near-infrared band; rRed is the reflectance value in visible red band. With the help of "Raster Calculator" tool of the "Spatial Analysis" extension of "ArcGIS" software package, the C-factor was calculated from NDVI, a spectral ratio between near infrared and red reflectance, extracted from satellite image. After the production of the NDVI image, the following formula was used to generate a C factor surface from NDVI values,[5]:

$$C = \exp (-a * NDVI / (b - NDVI)) \quad (11)$$

Where a and b are unit less parameters that determine the shape of the curve relating to NDVI and the C factor. A group researchers found that this scaling approach gave better results than assuming a linear relationship [5]. Finally, the values of 2 and 1 was selected for the parameters a and b, respectively, Since the C factor ranges from 0 (full cover) to 1 (bare land) and the NDVI values range from 1 (full cover) to 0 (bare land), the calculated NDVI values were inversed using the above equation.

3.5.5. Support Practice factor (P)

The soil loss of a specific practice relative to the soil loss incurred when plowing up and down the slope [2]. P value is equal to 1 when the land is plowed on the slope directly. This is also known as the worst practice. P value is lower and less than 1 when the adopted conservation practice reduces soil erosion. P values are chosen based on land use or soil management. The values of P factor based on land use within the project area have been determined as shown in Table 6.0.

Table 6: P factor for different land use within the project area [3].

| Landuse | P Factor |
|-------------------|----------|
| built up | 0.50 |
| Wetland | 0.60 |
| agricultural land | 0.10 |
| Bareland | 0.30 |
| Vegetation | 0.60 |

3.5.6. Final Calculations

Once raster layers for K, C, R, and LS have been created the last step is combining them together to make an erosion raster. This is done using The Raster Calculator under the Spatial Analyst tool. Raster calculator tool, part of the spatial analyst extension of the ArcGIS was used to calculate soil loss in the project area. The RUSLE equation was used to calculate the annual soil loss in sqkm/ha/year. The images produced were used as inputs and multiplied in the equation as follows: $R \times K \times LS \times C \times P = A$. The result of the equation was an image showing qualitative and quantitative volume of soil loss.

4.0. Results

4.1. Factor Maps

4.1.1. Potential Erosion Map

The input data were processed in ArcGIS and five factor maps: R, K, LS, C and P, were produced (Figures 9-17). These raster maps were integrated within the ArcGIS environment using the RUSLE relation to generate composite maps of the estimated erosion loss within the study area. Using a zonal statistics tool, an area-weighted mean of the potential erosion rates for the watershed was computed. Similarly, the erosion rates for slopes and LULC were generated to explore the relationship between slope and LULC on erosion. First, the slope map of the area was generated from DEM in ArcGIS and then reclassified into 5 classes. The erosion values for each class were thus obtained using zonal statistics. The results are presented in Figs 9-17 and tables 7.

The results showed that the Rainfall Erosivity Factor (R) value has been estimated at $(5023.83 \text{ MJ mm ha}^{-1} \text{ h}^{-1} \text{ yr}^{-1} - 5069.51 \text{ MJ mm ha}^{-1} \text{ h}^{-1} \text{ yr}^{-1})$ (Fig 13). Soil Erodibility Factor (K) value ranged from 0.027 to 0.30 $\text{ton.MJ}^{-1} \text{mm}^{-1}$ (Table 4). The topographic Factor (LS) value for the entire area ranged from 2.5 to 59.5 (Figure 15). The value of the Cover Management Factor (C) ranged between 0 and 0.45. The value indicates the percentage erosive capacity in comparison with bare fallow area. The highest value of 0.45 indicates that 45% of erosion occurs in the area in comparison with the bare fallow land (Figure 10). The Support Practice Factor (P) value ranged from 0.55 to 1 where a higher value indicates there is no support practice such that erosion is at its maximum due to the absence of any practice (Table 6).

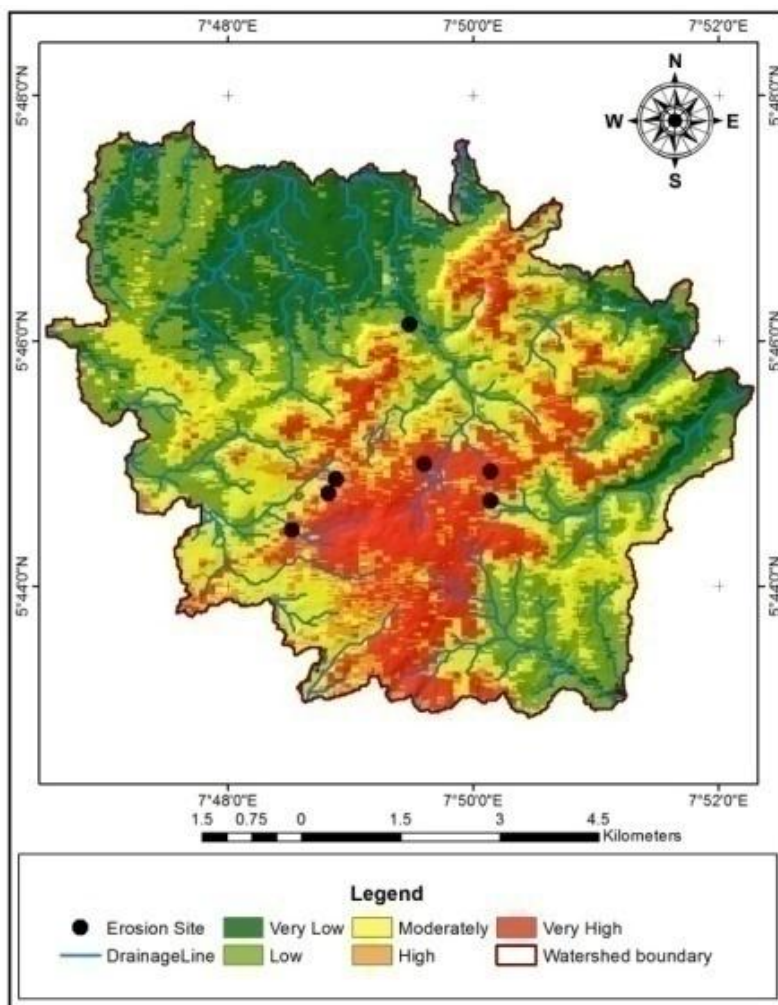


Figure 9: Vulnerability level map

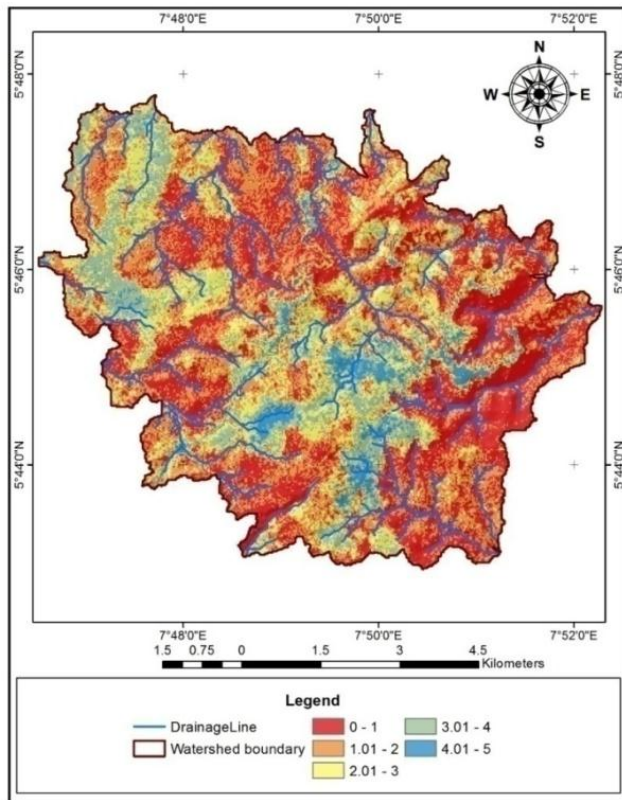


Figure 10: P factor Map (Land use and cover)

Table 7: Vulnerability Level in Erosion Risk classes (in sqkm)in the study area.

| Vulnerability Level | Range tonnes/hectare/year | Area (Sqkm) |
|---------------------|------------------------------|----------------|
| Very Low | 0 - 1,113.4861 | 15.5151 |
| Low | 1,113.4862 - 1,650.1563 | 23.8599 |
| Medium | 1,650.1564 - 2,365.7166 | 13.7187 |
| High | 2,365.7167 - 3,413.5014 | 4.0734 |
| Very high | 3,413.5015 - 6,889.0801 | 0.9864 |
| Total | | 58.1535 |

Table 9: Summary of results of soil analyses on samples from the Edda-Afikpo gully sites

| Sample location | Grain size distribution | | | Atterberg limits | | | Moisture content (%) | K (cm/s) | G _s | Shear strength | |
|-------------------------------|-------------------------|------|--------|------------------|----|----|----------------------|------------------------|----------------|-------------------------------------|--------------------|
| | Fines | Sand | Gravel | LL | PL | PI | | | | c _u (kN/m ²) | φ _u (°) |
| AliomaRoad | 14 | 85 | 1 | 25 | NP | NP | 7.4 | 1.630×10 ⁻³ | 2.37 | 36 | 13 |
| IgboroAmoji | 20 | 80 | 0 | 29 | NP | NP | 6.3 | 1.632×10 ⁻³ | 2.52 | 42 | 14 |
| Okagbue Road | 17 | 83 | 0 | 30 | NP | NP | 7.1 | 1.636×10 ⁻³ | 2.62 | 38 | 13 |
| Double Corner | 15 | 82 | 3 | 20 | NP | NP | 5.9 | 1.541×10 ⁻⁵ | 2.62 | - | - |
| Afikpo South Council old sec. | 5 | 94 | 1 | 21 | NP | NP | 6.3 | 1.544×10 ⁻³ | 2.59 | - | - |

Table 10: Soil characteristics and area coverage from RUSLE.

| Soil Type | Area Sqkm |
|---------------------|--------------|
| sandy loam surfaces | 43.589379 |
| clay surfaces | 16.313786 |

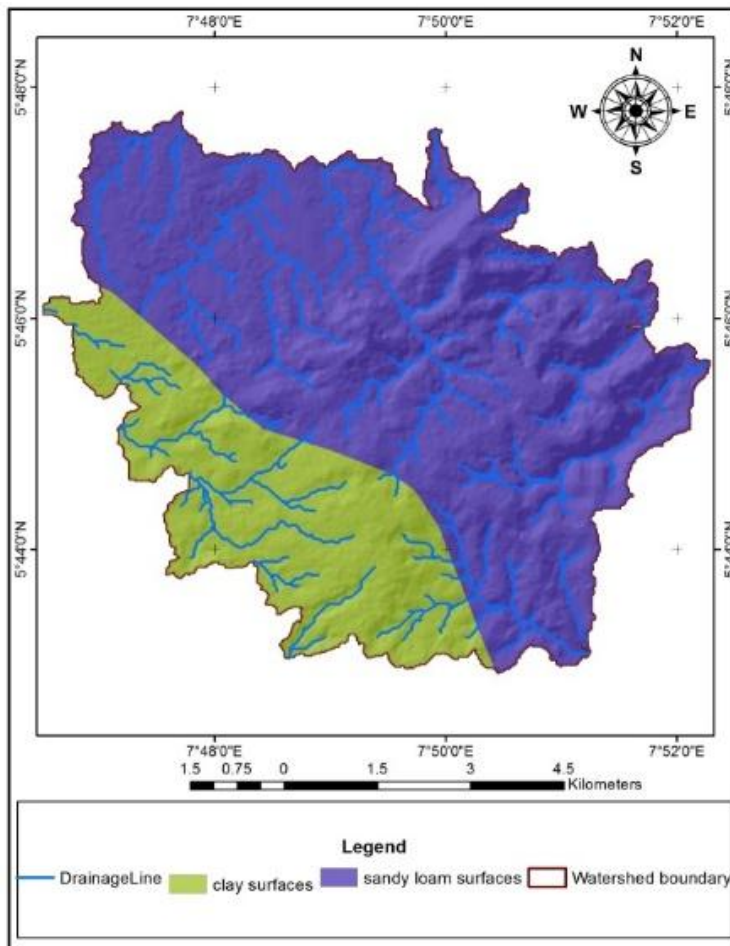


Figure 11: Soil types and characteristics

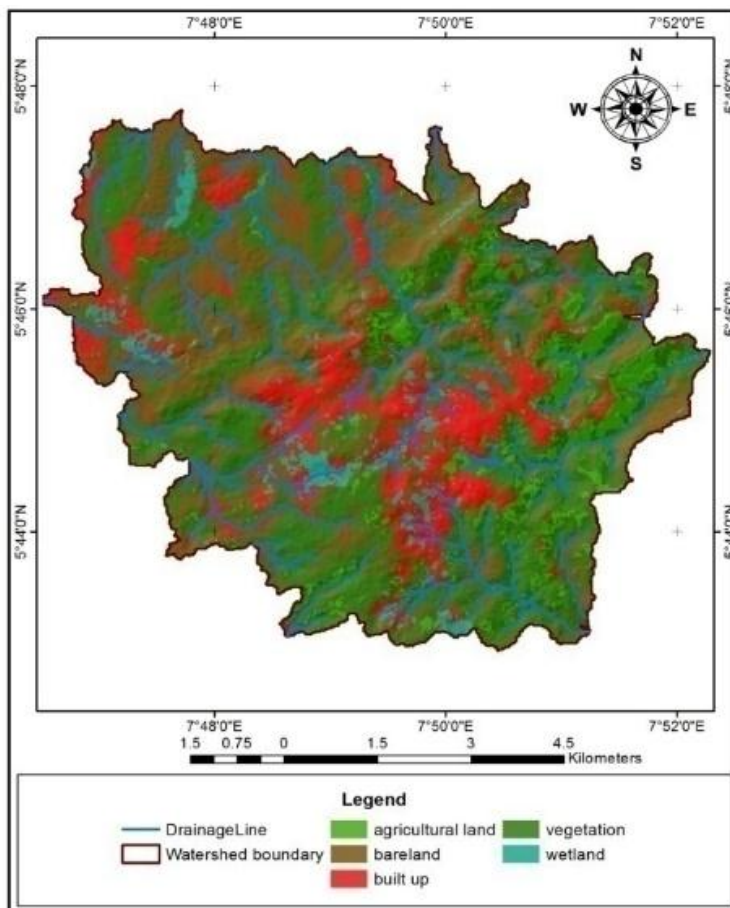


Figure 12: Land use classification

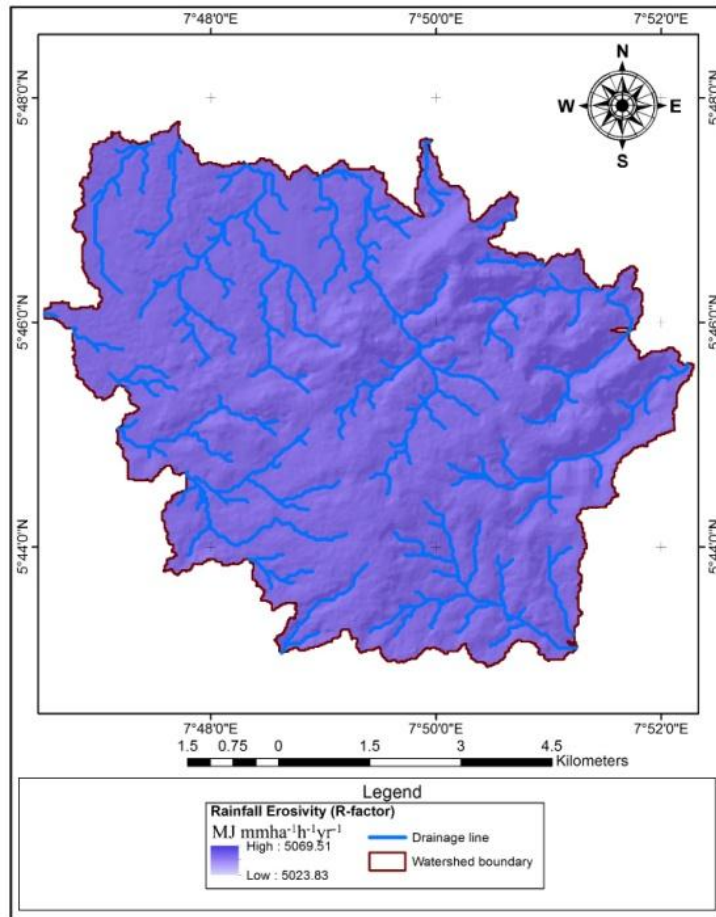


Figure 13: Soil erosivity factor

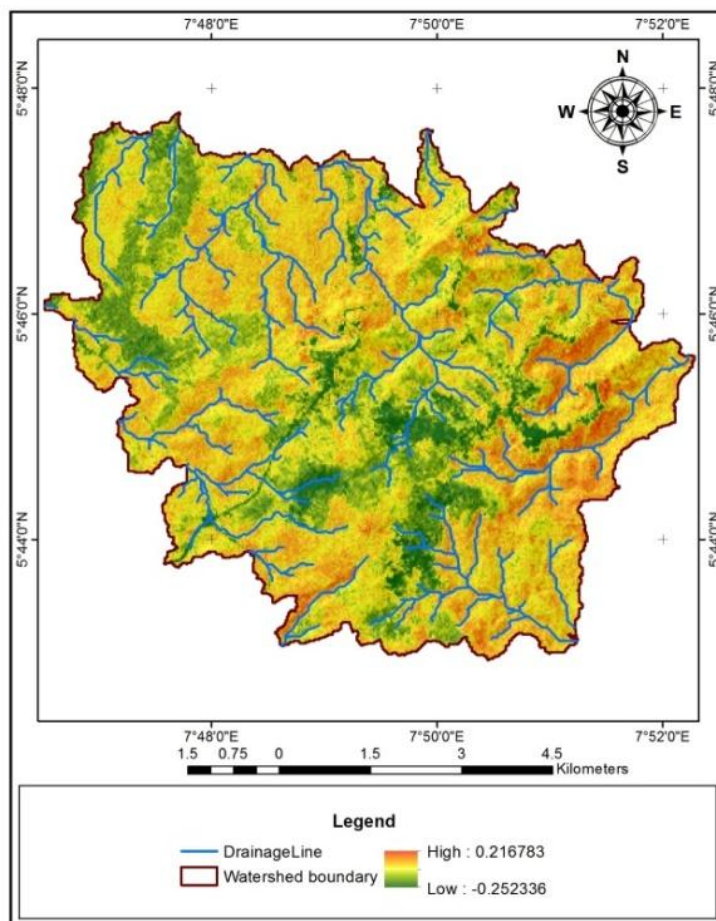


Figure 14: Vegetation index map

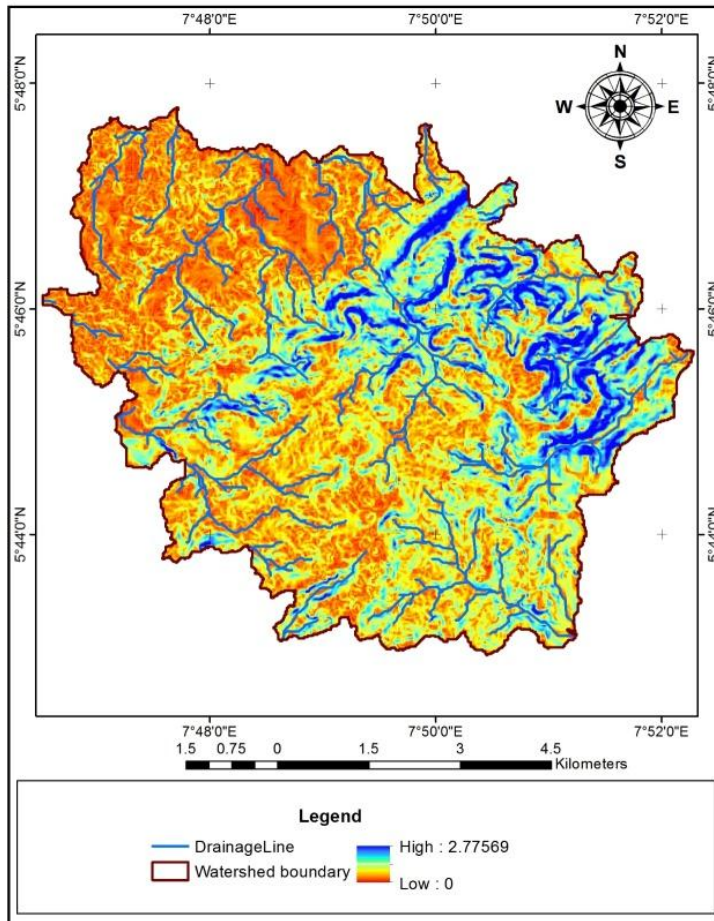


Figure 15: Slope length and gradient

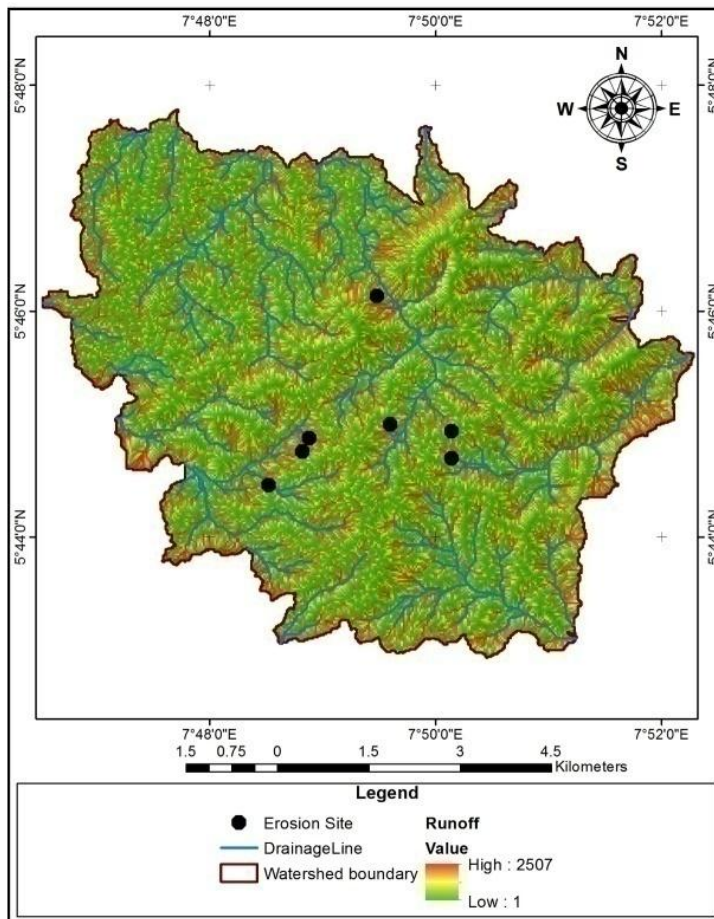


Figure 16: Erosion sites with run-off value

Table 8: Land use/Land cover classes within the project area

| Land cover Type | Area Sqkm |
|-------------------|-----------|
| built up | 9.0846 |
| Wetland | 2.5596 |
| agricultural land | 4.1238 |
| Bare land | 17.8245 |
| Vegetation | 26.3358 |

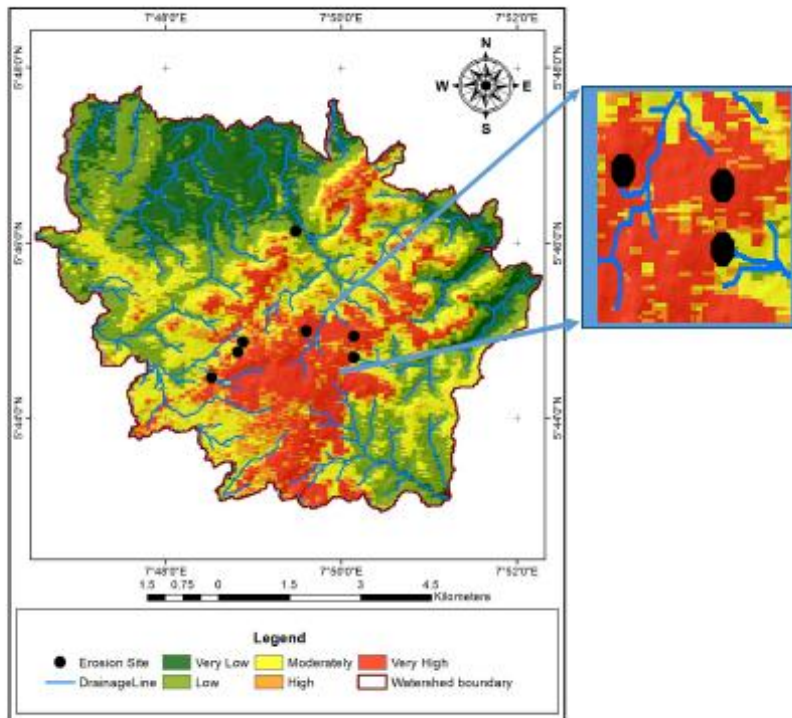


Figure 17: Validation of RUSLE

5.0. Discussions

For the purpose of soil loss estimation, the terrain is very suitable for application of RUSLE2. Types of erosion in the area include inter-rill and rill, ephemeral gullies, permanent, incised (classical) gullies, stream channels and mass movements. RUSLE2 is applicable to inter-rill and rill erosion, sediment yield from overland flow slope length, sediment yield from terrace channels and simple sediment control basins. Most applicable geographic regions are where rain occurs regularly and rainfall predominant means of precipitation, best soil medium to fine textured and slope length 50-300ft but 600ft-100ft acceptable. The purpose of the foregoing is to underscore the utility of the tools used in the study. The high risk areas in terms of erosion vulnerability correspond with the mesas (Fig 9).

5.1. Land use and cover management

These researchers submit that vegetation provides both hydrological and mechanical effects that generally are beneficial to slope stability. The land use pattern of any terrain is a reflection of the complex physical processes acting upon the surface of the earth, [3]. These processes include impact of climate, geologic and topographic conditions on the distribution of soils, vegetation and occurrence of water. The area is made up of settlements of predominantly farming communities. Farmlands exist alongside built up lands. From the study, it can be seen that the area of paved surfaces and man-made channels enormously contribute to the runoff volume. Developments are made at the slopes without adequate measures to channel storm waters downslope. Hence high runoff volumes on the fragile soil initiate rill erosion during high intensity rainfalls. Drainage lines mostly correspond with these construction sites and flows accumulate at these local cells to a certain threshold during intense storm events. A spatial perception of the land use classification is displayed in (Fig 12). The traditional farming communities embark on bush clearing and burning, often at the slopes. This lays bare the fragile soil and depletes the thin vegetation cover at the highlands. It is to be noted that vegetation cover in these areas comprises mainly heat-tolerant plant species like cashew. Deep-rooted plant species are scarce and occur at the incised valleys and gullies.

5.2. Soil index and geotechnical properties

The total area of the study is 59.9km² out of which 43.6km² is covered by sandy soils. These sandy soils contain very low moisture (5.9-7.4%), low shear strength, devoid of plasticity. All these index properties predispose the sediments to detachment and erosion. Based on the analysis, the amount of soil loss in the project area is about 1373.79 ton per year. As shown in the Fig 9 and Table 7, the amount of soil loss of each parcel of land in the basin ranges from 0 to 6889.08t/ha/year. Studies estimates mean monthly kinetic energy, using the equation by Wischmeier and Smith in the range of 1.5 to 87 MJ/ha; whereas the values ranged from 1.5 to 140 MJ/ha using the Kowal and Kassam equation [11,20]. The annual value of erosivity was 18510 MJ-mm/ha/h by

the EI index, 216 MJ/ha by the KE < 25 mm/h index and 1329 cm /h by the AI index.

Soil erosivity factor is high at the mesas (5023.83 MJ mm ha⁻¹ h⁻¹ yr⁻¹ - 5069.51 MJ mm ha⁻¹ h⁻¹ yr⁻¹) with a decreasing northward progression corresponding to the clay/shale surfaces [21]. In Fig 15, the high slope lengths and gradients and active erosion sites correspond with the built up areas and its proximity. In terms of vulnerability level in erosion risk, high to very high constitute 4.1% of the watershed which translate to 5.05km² of the 59km². This is very significant considering that it is concentrated around the settlements and bareland which make up only 9.08km² and 17.845km² of the watershed [22-25]. The implication of this is that the area left for future development, assuming total solution to this environmental hazard is 18.8% less.

Based on the model validation, 2 out of the 7 erosion sites falls within severely vulnerability level of the RUSLE result, while 3 and 2 of the erosion site falls within the very high and highly vulnerable areas respectively, which makes the erosion prediction map 85 percent accurate with real world phenomenon [26-28].

6.0. Conclusions

Efforts to contain soil erosion have been sustained at the local scale but far from adequate. Government institutions have been the main drivers of these efforts which have not been matched with education and enforcement of conservation and land use management practices among affected communities. The researchers therefore submit that a gap exists in the containment of environmental hazard management in Nigeria. The study has highlighted the main drivers of the environmental hazards. The process is facilitated by the Trifecta of hill slope hydrology, geology and land use practices. The emphasis to be made is the human factor component which appears to be reactive instead of proactive in the mitigation of these disasters. Since the residents are constrained to develop on drainage lines and slopes, concerted efforts must be made to develop a central storm water management system into which all runoffs must be channeled. Farmers should be educated on the need to explore the alternatives of cropping at the lowlands and copious wetlands and adopt practices that least predispose the area to sediment detachment and erosion. In this regard, bush burning must be totally eradicated while ridges must not run parallel to the slopes. Since some of these factors are natural, the residents must learn the environmental importance of forest canopy, revegetate and sustain existing forests. It is expected that the ministry of environment in Nigeria examine the outcomes of this research efforts for the management of soil erosion menace in Edda land.

References

- [1] G.E.K. Ofomata, "Soil Erosion in Nigeria: The Views of a Geomorphologist", University of Nigeria, Nsukka. Inaugural Lecture Series, 7 (43), pp. 43, 1987.
- [2] K.G. Renard, G.R. Foster, G.A. Weesies, D.K. McCool, D.C. Yoder, "Predicting soil erosion by water: A guide to conservation planning with the Revised Universal Soil Loss Equation (RUSLE)", Agriculture Handbook No. 703. U.S. Department of Agriculture, Agricultural Research Service, Washington, District of Columbia, USA, 1997.
- [3] T.J. Toy, G.R. Foster, K.G. Renard, "Soil Erosion: Processes, Prediction, Measurement, and Control", John Wiley & Sons, Inc., New York, 2002.
- [4] L.K. Schmitt, "Developing and Applying A Soil Erosion Model In: A Data-Poor Context To An Island In The Rural Philippines. Environ", Dev. Sust., 11(1), 19-42, 2009.
- [5] Z.Y. Wang, G. Wang, G. Huang, "Modeling of State Of Vegetation and Soil Erosion Overlarge Areas", International Journal of Sediment Research, 23, 181-196, 2008.
- [6] H.T. Soo, "Soil Erosion Modeling Using Rusle2And GIS On Cameron Highlands, Malaysia For Hydropower Development, A Master's thesis done at RES", The School for Renewable Energy Science, 2011.
- [7] R. Anbalagan, "Landslide hazard evaluation and zonation mapping in mountainous terrain", Engineering Geology (Elsevier), Vol. 32, Issue 4, pp. 269-277, 2003.
- [8] D.H. Gray, and A.T. Leiser, "Biotechnical slope protection and erosion control", Van Nostrand Reinhold: New York, N.Y, 1982.
- [9] D.R. Greenway, "Vegetation and slope stability", In Slope Stability, edited by M. F. Anderson and K. S. Richards, Wiley and Sons, New York, 1987.
- [10] CIAT-CSI SRTM, "Digital elevation map of Afikpo area", Retrieved from: <http://srtm.csi.cgiar.org>; on 20 June, 2017.
- [11] F.K. Salako, B.S. Ghuman, R. Lal, "Rainfal erosivity in south central Nigeria", Soil Technology, 7, Pp. 279-290, 1995.
- [12] S.A. Schumm, "Evolution of drainage systems & slopes in Badlands at Perth Anboy, New Jersey", Bulletin of the Geological Society of America, 67, pp.597-646, 1956.
- [13] R.E. Horton, 1945. Erosional development of streams and their drainage basins, Bulletin of the Geological Society of America, Vol. 56, pp. 275-370, 1945.
- [14] H.S. Kim, "Soil Erosion Modeling Using RUSLE and GIS on the IMHA Watershed", South Korea, pp. 20- 77. Doctoral dissertation, Department of Civil Engineering. Colorado State University Fort Collins, Colorado Spring 2006.
- [15] T. Sudeep, K. Pooja, "Estimation of soil erosion in Nepal using RUSLE Modeling and Geospatial Tool", Geosciences (Switzerland), 2019.
- [16] F.K. Salako, "Development of isoerodent maps for Nigeria from daily rainfall amount", Geoderma, 156, 372-378, 2010.
- [17] M. Kouli, P. Souplos, and F. Vallianatos, "Soil erosion prediction using the revised universal soil loss equation (RUSLE) in a GIS framework, Chania, Northwestern Crete, Greece", Environ Geol., 57, 483-497, 2009.
- [18] D.K. McCool, L.C. Brown, G.R. Foster, C.K. Mutchler, and L.D. Meyer, "Revised slope steepness factor for the Universal Soil Loss Equation Trans", Am. Soc. Agric. Eng., 30 (5), pp. 1387-1396, 1987.
- [19] R. Remortel Van, M. Hamilton, R. Hickey, "Estimating the LS factor for RUSLE through iterative slope length processing of digital 16. Elevation data", Cartography, 30 (1), pp. 27-35, 2001.
- [20] J.G. Lyon, (Ed.), "GIS for Water Resources and Watershed Management". CRC Press, Washington D.C, 2003.

- [21] F.C. Dai, C.F. Lee, and Y.Y. Nagi, "Landslide risk assessment and management: an overview", *Engineering Geology*, Vol. 64, pp. 65-87, 2002.
- [22] G.T. Amangabara, "Analysis of Selected Failed Gully Erosion Control Works in Imo State.In: *Hydrology for Disaster Management*", Special Publication of the Nigerian Association of Hydrological Sciences, 2012.
- [23] M.N. Fausta, "Hydrological information for Dam site selection by Integrating Geographic Information System (GIS) and Analytical Hierarchical Process (AHP)", 2015.
- [24] R.E. Horton, "Drainage basin characteristics, *Transactions*", American Geophysical Union, Vol. 13, pp. 350-61, 1932.
- [25] M.J. Kirky, "Modelling the Link between vegetation and landforms", *Geomorphology*, 13, 319-335, 1995.
- [26] D.R. Maidment, "Arc Hydro:GIS for water resources", Redlands, Calif.:ESRI press, 2002.
- [27] A.N. Strahler, "Quantitative analysis of watershed geomorphology", *Transactions of the American Geophysical Union*, 38(6), 913-920, 1957.
- [28] K. Terzaghi, "Mechanism of landslides. Berkey volume: Application of geology to engineering practice", Geological Society of America, New York, pp83-123, 1950.